

## Enhancement of Optical Absorption, Photoluminescence and Raman Transitions in $\text{Bi}_2\text{O}_3\text{-GeO}_2$ Glasses with Embedded Silver Nanoparticles

Maylon M. Martins,<sup>a</sup> Diego S. Silva,<sup>a,b</sup> Luciana R. P. Kassab,<sup>\*,a</sup> Sidney J. L. Ribeiro<sup>c</sup> and Cid B. de Araújo<sup>d</sup>

<sup>a</sup>Faculdade de Tecnologia de São Paulo, CEETEPS/UNESP, 01124-060 São Paulo-SP, Brazil

<sup>b</sup>Departamento de Engenharia de Sistemas Eletrônicos, Escola Politécnica da USP, 05508-900 São Paulo-SP, Brazil

<sup>c</sup>Instituto de Química, Universidade Estadual Paulista-UNESP, CP 355, 14870-90 Araraquara-SP, Brazil

<sup>d</sup>Departamento de Física, Universidade Federal de Pernambuco, 50670-901 Recife-PE, Brazil

The influence of silver nanoparticles (Ag-NPs) on the optical properties of  $\text{Bi}_2\text{O}_3\text{-GeO}_2$  glasses was investigated aiming the characterization of their potential for applications in photonic devices. The samples were prepared by the melt-quenching technique starting from high purity oxides ( $\text{GeO}_2$ ,  $\text{Bi}_2\text{O}_3$  and  $\text{AgNO}_3$ ). Heat-treatment during different times was performed to nucleate Ag-NPs. A transmission electron microscope was used to confirm the presence of Ag-NPs and to determine their sizes and composition. The glass network was studied by spontaneous Raman scattering. The optical absorption spectra showed an absorption band at ca. 500 nm associated to the bismuth ions, and a 7-fold enhancement of absorption was observed in the samples with Ag-NPs. Photoluminescence (PL) spectra were obtained by exciting the samples with a 808 nm laser. Maximum enhancements of ca. 100% of the PL band centered at 1300 nm and ca. 70% of the Raman spectrum were observed due to the nucleation of the Ag-NPs. The enhanced optical response of the samples with Ag-NPs is attributed to the growth of the local field on the isolated bismuth ions and clusters that are located in the vicinity of the nanoparticles. The results illustrate the large potential of  $\text{Bi}_2\text{O}_3\text{-GeO}_2$  with Ag-NPs to be used in photonic devices.

**Keywords:** heavy metal oxide glass, silver nanoparticle, germanate glass, infrared photonic device

### Introduction

Heavy metal oxide (HMO) glasses are attracting large attention because of their linear and nonlinear optical properties that make them ideal candidates for applications such as ultrafast optical switches, optical limiters and active photonic devices.<sup>1-18</sup> In general, besides low optical absorption in the visible and in the near-infrared (NIR) regions, the HMO glasses present high index of refraction (ca. 2.0), low cutoff phonon energies (ca. 800  $\text{cm}^{-1}$ ), large polarizability, large resistance to moisture and good thermal stability that allow the fabrication of optical fibers. Particularly, the glasses containing bismuth oxide ( $\text{Bi}_2\text{O}_3$ ) deserve large attention because of the broadband photoluminescence (PL) from 1000 to 1600 nm, due to bismuth (Bi) ions.<sup>12-17</sup> Ren *et al.*,<sup>14,15</sup> for instance, reported

efficient optical amplification in the region 1272-1348 nm using Bi-doped magnesium-germanate,<sup>14</sup> and Bi-doped germano-silicate glasses,<sup>15</sup> and Dianov *et al.*<sup>18</sup> demonstrated laser action between 1150 and 1300 nm in a Bi-doped aluminosilicate fiber.<sup>18</sup> The NIR broadband emission was also observed in a Bi-doped soda-lime silicate,<sup>16</sup> and chalcogenide glass.<sup>17</sup> Therefore new possibilities for optical communications using optical fibers containing bismuth in comparison with the results already reported with rare-earth ions doped fibers are envisaged.

In the present work we investigate the influence of silver nanoparticles (Ag-NPs) on the optical properties of  $\text{Bi}_2\text{O}_3\text{-GeO}_2$  glasses. The main motivation for this work was to obtain a composite material with enhanced optical properties in comparison with the well-known  $\text{Bi}_2\text{O}_3\text{-GeO}_2$  glass. The results showed a 7-fold enhanced absorption in the visible range, PL growth of ca. 100% at 1300 nm as well as a ca. 70% enhancement of the spontaneous Raman

\*e-mail: kassablm@osite.com.br

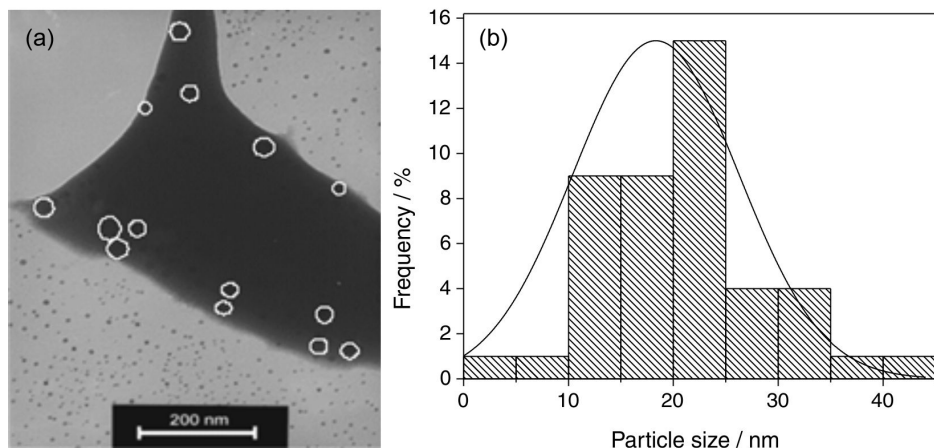


**Figure 1.** (a) TEM image of  $89.6\text{GeO}_2\text{-}9.6\text{Bi}_2\text{O}_3\text{-}0.8\text{AgNO}_3$  (mol%) glass with Ag-NPs, heat treated during 1 hour at  $420\text{ }^\circ\text{C}$ ; (b) size distribution of the Ag-NPs.

scattering cross-section due to the presence of the Ag-NPs. In the Experimental section we describe the methods and techniques used for fabrication and characterization of the glasses. In the Results and Discussion section we report on the structural and optical properties of the samples. Finally, in the Conclusions, we present a summary of the results.

## Experimental

The samples investigated were fabricated using the melt-quenching method with the starting composition (in mol%):  $89.6\text{GeO}_2\text{-}9.6\text{Bi}_2\text{O}_3\text{-}0.8\text{AgNO}_3$ . The reagents were melted in an alumina crucible for 1 h at  $1200\text{ }^\circ\text{C}$ , quenched in a preheated brass mold, annealed at  $420\text{ }^\circ\text{C}$  during 1 h (to avoid internal stress) and cooled to room temperature inside the furnace. After this procedure, the samples were polished and cut in order to have parallel faces. The samples prepared with  $\text{AgNO}_3$  were heat-treated (HT) during 1, 12 and 24 h at  $420\text{ }^\circ\text{C}$  to thermally reduce the  $\text{Ag}^+$  ions to  $\text{Ag}^0$  and to nucleate the Ag-NPs. The melting temperature of  $1200\text{ }^\circ\text{C}$  was chosen based on our previous experiments that showed higher NIR luminescence when compared to the emission from the samples melted at  $1100\text{ }^\circ\text{C}$ . Samples with composition (in mol%):  $86\text{GeO}_2\text{-}14\text{Bi}_2\text{O}_3$  and  $80.4\text{GeO}_2\text{-}19.6\text{Bi}_2\text{O}_3$  were also prepared, without Ag-NPs, and melted at  $1100\text{ }^\circ\text{C}$  and  $1200\text{ }^\circ\text{C}$ , for comparison with the optical response of the glass containing Ag-NPs.

A 200 kV transmission electron microscope (TEM) was used to determine the sizes and shapes of the Ag-NPs. Energy dispersive X-ray spectroscopy was performed during the TEM analysis in order to confirm the presence of Ge, Bi and Ag-NPs. Electron diffraction measurements were performed to determine the crystalline structure of Bi NPs according to JCPDS-ICDD data base.<sup>19</sup> For these measurements the samples were milled, mixed with distilled water, and partially decanted. The floating part was

taken by using a metallic screen and analyzed by TEM.

The linear optical absorption spectra were measured with a spectrophotometer operating from 350 to 1600 nm. The PL measurements were made by exciting the samples with a 808 nm continuous-wave diode laser (maximum power: 200 mW). A spectrometer, attached to a photomultiplier and a computer, was used to analyze the PL signals. Spontaneous Raman scattering measurements using a laser operating at 532 nm were performed to study the glass network. All measurements were made with the samples at room temperature.

## Results and Discussion

The TEM images obtained for samples HT during 1 h showed the presence of Ag-NPs with average diameter of ca. 20 nm. One representative TEM image is shown in Figure 1a and the size distribution of the NPs is shown in Figure 1b.

Figure 2 shows energy dispersive spectroscopy (EDS) results that confirm the presence of Ge, Bi and Ag in the samples. The features corresponding to the Cu K line are

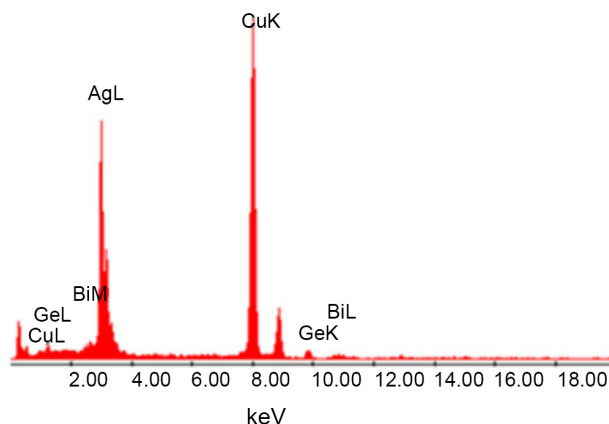


**Figure 2.** EDS spectrum of the  $89.6\text{GeO}_2\text{-}9.6\text{Bi}_2\text{O}_3\text{-}0.8\text{AgNO}_3$  (mol%) glass sample heat-treated during 1 hour at  $420\text{ }^\circ\text{C}$ .

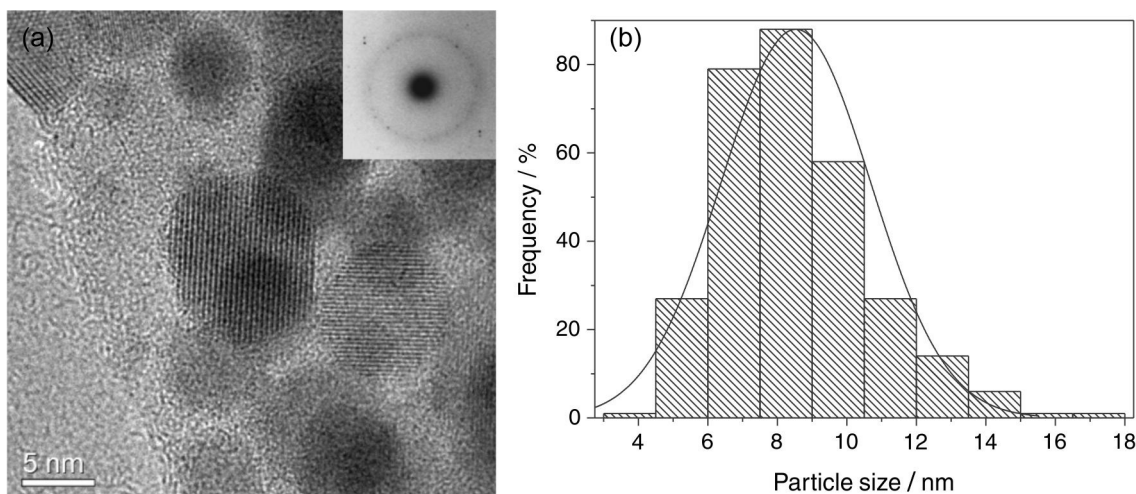
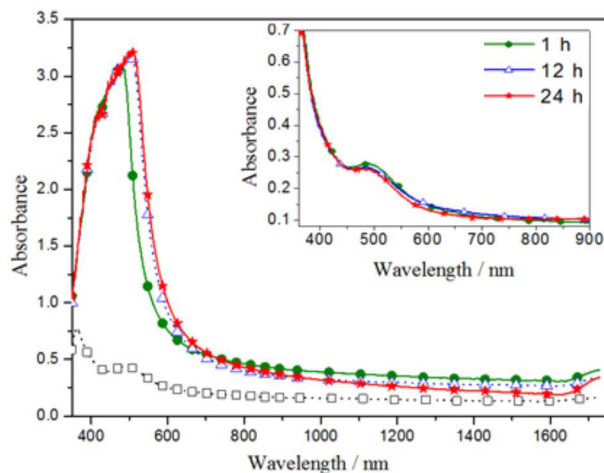


**Figure 3.** (a) TEM image of 89.6GeO<sub>2</sub>-9.6Bi<sub>2</sub>O<sub>3</sub>-0.8AgNO<sub>3</sub> (mol%) glass without Ag-NPs. The Bi particles observed were formed several minutes after the exposition to the electron beam irradiation. The inset shows the diffraction pattern that confirms the rhombohedral structure of bismuth; (b) size distribution of the Bi particles.

due to the grid where the sample is placed for the TEM measurements.

Figure 3a shows a TEM image of Bi NPs that present rhombohedral structure in agreement with literature.<sup>19</sup> This measurement was made with samples without Ag-NPs. The inset of Figure 3a shows the pattern that was used to calculate the diffraction indices (104 and 110) of the Bi structure according to the JCPDS-ICDD data base.<sup>20</sup> The Bi NPs size distribution is presented in Figure 3b and shows average dimensions of ca. 9 nm. We recall that the formation of Bi NPs and Bi clusters due to electron beam irradiation in a TEM was previously reported.<sup>19</sup> In the present study this effect was observed several minutes after starting the irradiation; motion of Bi NPs was noted where the electron beam was focused as well as a tendency of coalescence.

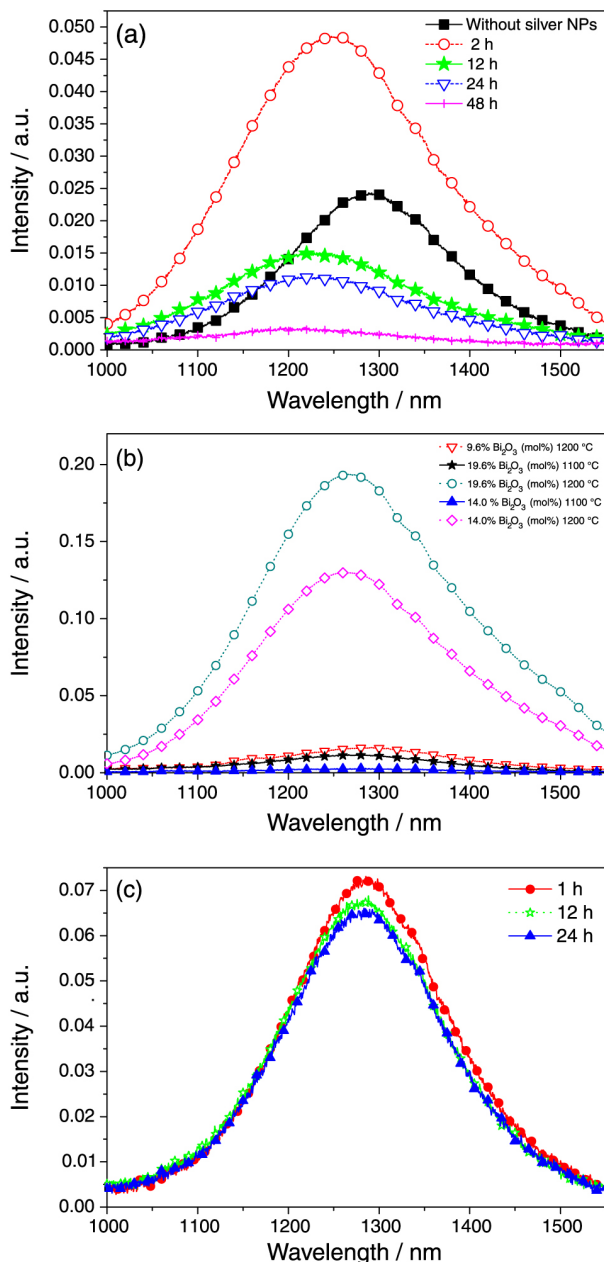
The absorption spectra of the samples prepared with and without Ag-NPs are shown in Figure 4. Notice that the sample without Ag-NPs presents a band centered at ca. 500 nm related to divalent bismuth ions (Bi<sup>2+</sup>), as reported for other Bi-doped glasses.<sup>21,22</sup> The spectra of the samples with AgNO<sub>3</sub> in the starting composition present a large broadband in the blue-orange region with an amplitude that increases with the increase of the heat-treatment time. This behavior is due to the localized surface plasmons band associated to the Ag-NPs, but it is also possible that the Bi<sup>2+</sup> located in the vicinity of the Ag-NPs are also contributing due to the enhancement of their absorption transitions centered at ca. 500 nm. The 7-fold increase observed in the absorption band is an evidence of the large volume fraction of the Ag-NPs. The inset in Figure 4 illustrates the behavior of the samples without Ag-NPs, heat-treated during 1, 12 and 24 hours. It can be seen a small decrease of the Bi<sup>2+</sup> absorption band as reported for other bismuth doped glasses;<sup>21,23</sup> this change is



**Figure 4.** Room temperature absorption spectra of the 89.6GeO<sub>2</sub>-9.6Bi<sub>2</sub>O<sub>3</sub>-0.8AgNO<sub>3</sub> (mol%) glass. The inset shows the behavior of the sample without Ag-NPs for different heat-treatment times. Sample heat-treated during: 1 h (solid circles); 12 h (triangles); 24 h (asterisks). The spectrum of the sample without Ag-NPs is shown for reference (squares). Samples thickness: 2.0 mm.

negligible in comparison with the large increase observed for the samples with Ag-NPs.

Figure 5 presents the PL spectra of the samples excited at 808 nm. The strong band from 1000 to 1600 nm, centered at 1300 nm, is attributed to the Bi<sup>3+</sup> luminescence centers. A red-shift of the NIR band in the samples with Ag-NPs can be observed in Figure 5a. For the sample HT during 1 h the NIR band shifted to ca. 1250 nm, whereas for longer heat treatment times the band shifted to ca. 1220 nm. This effect is probably related to changes of the local environment of bismuth in the glass structure, due to the nucleation of Ag-NPs. Analogous behavior was observed in previous work<sup>23</sup> where a shift of the NIR band was attributed to changes in the glass structure.



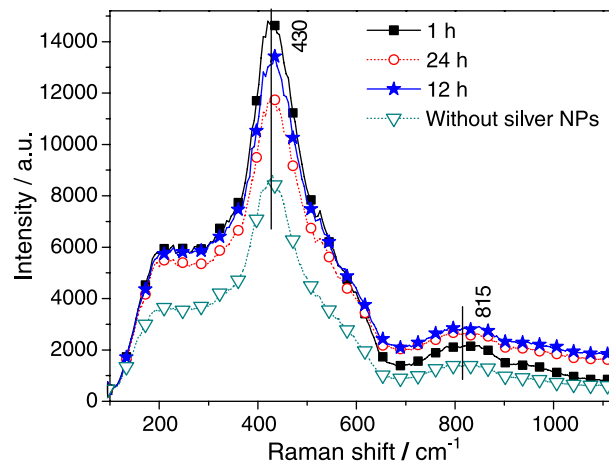
**Figure 5.** (a) Photoluminescence (PL) spectra of the  $89.6\text{GeO}_2\text{-}9.6\text{Bi}_2\text{O}_3\text{-}0.8\text{AgNO}_3$  (mol%) glass excited at 808 nm, for different heat-treatment intervals. The sample without Ag-NPs is shown for reference; (b) results of  $90.4\text{GeO}_2\text{-}9.6\text{Bi}_2\text{O}_3$ ,  $86\text{GeO}_2\text{-}14\text{Bi}_2\text{O}_3$  and  $80.4\text{GeO}_2\text{-}19.6\text{Bi}_2\text{O}_3$  glasses (mol%), without Ag-NPs, melted at 1100 and 1200 °C; (c) behavior of the PL spectra for the sample without Ag-NPs for three heat-treatment time intervals.

Figure 5b shows the results for  $\text{GeO}_2\text{-Bi}_2\text{O}_3$  glasses prepared without Ag-NPs, melted at 1100 and 1200 °C. Notice that the samples melted at 1200 °C present larger NIR emission that indicates a larger number of  $\text{Bi}^{3+}$  centers. This was the reason for the choice of the 1200 °C melting temperature in the present work.

Figure 5a exhibits ca. 100% enhancement of the PL intensity at ca. 1300 nm when a comparison between the

sample HT during 1 h and the sample without Ag-NPs is made. The PL enhancement is attributed to the local field growth in the vicinity of the Ag-NPs. For the samples HT during longer times quenching was observed probably due to the larger number of Ag-NPs nucleated and the reduction of the distances between the Ag-NPs and the luminescence centers. The PL quenching should not be attributed to the oxidation of  $\text{Bi}^{3+}$  because the change observed in the samples without Ag-NPs HT during 12 and 24 h is negligible, as illustrated by Figure 5c.

Figure 6 presents the Raman spectra for the samples with and without Ag-NPs. The shoulder in the region from 200 to 300  $\text{cm}^{-1}$  may be attributed to the asymmetric motion of Bi atoms that are simultaneously half-bridged and half-nonbridged to oxygen (O-Bi-O).<sup>24,25</sup> The band at ca. 430  $\text{cm}^{-1}$  is assigned to the symmetric stretching of bridged oxygen in bisecting the Ge-O-Ge plane in predominantly six-membered rings.<sup>26</sup> The Raman band centered at 815  $\text{cm}^{-1}$  is related to the asymmetric vibration of the nonbridging oxide structures,  $\text{Ge-O}^-$  and B-O. The Raman signal due to the  $\text{GeO}_4^{2-}$  vibration is expected to be dominant in the present case.<sup>23</sup> For the samples with Ag-NPs, the maximum enhancement of ca. 70% was observed due to the enhanced local electromagnetic field in the interface between the Ag-NPs and the dielectric medium, the so-called surface enhanced Raman scattering (SERS) effect.<sup>27</sup>



**Figure 6.** Raman spectra of the glass  $89.6\text{GeO}_2\text{-}9.6\text{Bi}_2\text{O}_3\text{-}0.8\text{AgNO}_3$  (mol%) heat-treated during 1, 12 and 24 h, at 420 °C. The spectrum for the sample without Ag-NPs is shown for reference (laser wavelength: 532 nm).

## Conclusions

This is the first report that shows the influence of silver nanoparticles on the absorption spectrum, near-infrared luminescence and Raman vibrational modes of the  $\text{Bi}_2\text{O}_3\text{-GeO}_2$  glass. The results show that this glass containing Ag-NPs has large potential to be used for

color filters in the blue-orange spectral region as well as for devices requiring intense and large bandwidth luminescence in the 1200-1600 nm region. The 7-fold increase observed for the linear absorption band in the blue-orange region and the ca. 100% enhancement in the NIR luminescence demonstrate the important role of Ag-NPs for the optical performance of this material. Surface enhanced Raman scattering due to the influence of the Ag-NPs was also observed.

## Acknowledgements

We acknowledge financial support by the Conselho Nacional de Desenvolvimento Científico e Tecnológico (CNPq) and Fundação de Amparo a Ciência e Tecnologia do Estado de Pernambuco (FACEPE). The work was performed in the framework of the National Institute of Photonics (INCT de Fotônica) project. We acknowledge the Nanotechnology National Laboratory (LNNano), CNPEM-Campinas/Brazil, for the HR-TEM measurements, and Laboratório de Microeletrônica/EPUSP, for the Raman measurements.

## References

- Sun, H. T.; Fujii, M.; Sakka, Y.; Bai, Z.; Shirahata, N.; Zhang, L.; Miwa, Y.; Gao, H.; *Opt. Lett.* **2010**, *35*, 1743.
- Meng, X. G.; Qiu, J. R.; Peng, M. Y.; Chen, D. P.; Zhao, Q. Z.; Jiang, X. W.; Zhu, C. S.; *Opt. Express* **2005**, *13*, 1628.
- Hasegawa, T.; Nagashima, T.; Sugimoto, M.; *Opt. Commun.* **2005**, *250*, 411.
- Kassab, L. R. P.; da Silva, D. S.; de Almeida, R.; de Araújo, C. B.; *Appl. Phys. Lett.* **2009**, *94*, 101912.
- Kassab, L. R. P.; da Silva, D. S.; de Araújo, C. B.; *J. Appl. Phys.* **2010**, *107*, 113506.
- Manzani, D.; de Araújo, C. B.; Boudebs, G.; Messaddeq, Y.; Ribeiro, S. J. L.; *J. Phys. Chem. B* **2013**, *117*, 408.
- Oliveira, T. R.; Falcão-Filho, E. L.; de Araújo, C. B.; da Silva, D. S.; Kassab, L. R. P.; da Silva, D. M.; *J. Appl. Phys.* **2013**, *114*, 073503.
- de Araújo, C. B.; da Silva, D. S.; de Assumpção, T. A. A.; Kassab, L. R. P.; da Silva, D. M.; *The Sci. World J.* **2013**, 385193.
- da Silva, D. S.; Naranjo, L. P.; Kassab, L. R. P.; de Araújo, C. B.; *Appl. Phys. B* **2012**, *106*, 1015.
- Rulkov, B.; Ferin, A. A.; Popov, S. V.; Taylor, J. R.; Razdobreev, I.; Bigot, L.; Bouwmans, G.; *Opt. Express* **2007**, *15*, 5473.
- Fujimoto, Y.; Nakatsuka, M.; *Appl. Phys. Lett.* **2003**, *82*, 3325.
- Peng, M.; Qin, J.; Chen, D.; Meng, X.; Yang, L.; Jiang X.; Zhu, C.; *Opt. Lett.* **2004**, *29*, 1998.
- Peng, M.; Qiu, J.; Chen, D.; Meng, X.; Zhu, C.; *Opt. Lett.* **2005**, *30*, 2433.
- Ren, J.; Wu, B.; Jiang, X.; Dong, H.; Zeng, H.; Qin, J.; *Appl. Phys. B* **2007**, *88*, 363.
- Ren, J.; Dong, H.; Zeng, H.; Hu, H.; Zhu, C.; Qin, J.; *IEEE Photonics Technol. Lett.* **2007**, *19*, 1395.
- Arai, Y.; Suzuki, T.; Ohishi, Y.; Morimoto, S.; Khonton, S.; *Appl. Phys. Lett.* **2007**, *90*, 261110.
- Hughes, M. A.; Akada, T.; Suzuki, T.; Ohishi, Y.; Hewak, D. W.; *Opt. Express* **2009**, *17*, 19345.
- Dianov, C. M.; Dvoyrin, V. V.; Mashinsky, V. M.; Umnikov, A. A.; Yaskov, M. V.; Guryanov, A. N.; *Quantum Electron.* **2005**, *35*, 1083.
- Sepulveda-Guzman, S.; Elizondo-Villarreal, N.; Ferrer, D.; Castro, A. T.; Gao, X.; Zhou, J. P.; Yacaman, M. J.; *Nanotechnology* **2007**, *18*, 335604
- JCPDS International Centre for Diffraction Data 2003 PDF 85-1330; PCPDFWIN v. 24.
- Guo, X.; Li, H. J.; Su, L. B.; Yu, P. S.; Zhao, H. Y.; Liu, J. F.; Xu, J.; *Laser Phys.* **2011**, *21*, 901.
- Miller, A. E.; Nassau, K.; Lyons, K. B.; Lines, M. E.; *J. Non-Cryst. Solids* **1988**, *99*, 289.
- Jiang, X.; Su, L.; Guo, X.; Tang, H.; Fan, X.; Zhan, Y.; Wang, Q.; Zheng, L.; Li, H.; Xu, J.; *Opt. Lett.* **2012**, *37*, 4260.
- Yu, Q.; Chen, F.; Xu, T.; Dai, S.; Zhang, Q.; *J. Non-Cryst. Solids* **2013**, *378*, 254.
- Baia, L.; Kiefer, W.; Simon, S.; Ruman; *Rep. Phys.* **2004**, *56*, 430.
- Durben, D. J.; Wolf, G. H.; *Phys. Rev. B* **1991**, *43*, 2355.
- Dousti, M. R.; Sahar, M. R.; Amjad, R. J.; Ghoshal, S. K.; Awang, A.; *J. Lumin.* **2013**, *143*, 368.

Submitted: June 27, 2015

Published online: July 31, 2015

FAPESP has sponsored the publication of this article.